THE JOURNAL OF BIOLOGICAL CHEMISTRY VOL. 287, NO. 8, pp. 5784–5796, February 17, 2012


# Dimerization and Cytoplasmic Localization Regulate Hippo Kinase Signaling Activity in Organ Size Control*[S]

Received for publication, October 4, 2011, and in revised form, December 22, 2011 Published, JBC Papers in Press, January 3, 2012, DOI 10.1074/jbc.M111.310334

**Yunyun Jin[‡], Liang Dong[‡], Yi Lu[‡], Wenqing Wu[‡], Qian Hao[‡], Zhaocai Zhou[‡], Jin Jiang[§], Yun Zhao[‡1], and Lei Zhang[‡2]**

*From the [‡]State Key Laboratory of Cell Biology, Institute of Biochemistry and Cell Biology, Shanghai Institutes for Biological Sciences, Chinese Academy of Sciences, 320 Yue-Yang Road, Shanghai 200031, China and the [§]Department of Developmental Biology, University of Texas Southwestern Medical Center, Dallas, Texas 75390*

**Background:** Hippo plays critical roles in organ size control, and the regulation of its activity remains poorly characterized.
**Results:** N-terminal dimerization of Hpo is critical for Hippo kinase activity. The Hippo C-terminal half promotes cytoplasmic localization and activity of Hippo.
**Conclusion:** Dimerization and nucleocytoplasmic translocation of Hippo are crucial for its biological function.
**Significance:** Dimerization and cytoplasmic localization regulate Hippo activity.

**The Hippo (Hpo) signaling pathway controls organ si e by regulating the balance between cell proliferation and apoptosis. Although the Hpo function is conserved, little is known about the mechanism of how its kinase activity is regulated. Based on structural information, we performed mutation-function analysis and provided *in vitro* and *in vivo* evidence that Hpo activation requires proper dimeri ation of its N-terminal kinase domain as well as the C-terminal SARAH domain. Hpo carrying point mutation M242E can still dimeri e, yet the dimers formed between intermolecular kinase domains were altered in conformation. As a result, autophosphorylation of Hpo at Thr-195 was blocked, and its kinase activity was abolished. In contrast, Hpo carrying I634D, a single mutation introduced in the Hpo C-terminal SARAH domain, disrupted the dimeri ation of the SARAH domain, leading to reduced Hippo activity. We also find that the Hpo C-terminal half contains two nuclear export signals that promote cytoplasmic locali ation and activity of Hpo. Taken together, our results suggest that dimeri ation and nucleocytoplasmic translocation of Hpo are crucial for its biological function and indicate that a proper dimer conformation of the kinase domain is essential for Hpo autophosphorylation and kinase activity.**

Restriction of tissue growth is an important means by which the developmental program generates an organism of a defined size and form (1). Studies in the last decade have unveiled a critical role for the evolutionarily conserved Hpo signaling pathway in restricting tissue growth by controlling cell proliferation and death (2–5). Recent studies in *D* and mammals have demonstrated links between the Hpo signaling network and other established signaling cascades, such as Wnt/wingless, Hedgehog, BMP/dpp, and Jun kinase (6–10), suggesting that the Hpo pathway acts via cell-autonomous or non-cell-autonomous mechanisms in various physiological contexts during animal development (11–13). Furthermore, aberrant signaling of the Hpo pathway is also linked to a range of diseases, most notably cancer (14).

Initially discovered by genetic screens in *D* for tumor suppressor genes, the core Hpo pathway comprises a kinase cascade: the serine/threonine Ste20-like kinase Hpo, the nuclear Dbf2-related (NDR) family protein kinase Warts (Wts), the WW domain scaffolding protein Salvador (Sav), and Mob-as-tumor-suppressor (Mats). Together with Sav, activated Hpo phosphorylates the Wts-Mats kinase complex (15–20), which triggers the kinase phosphorylation cascade and inhibits the transcriptional activity of the downstream transcription complex: scalloped (Sd), a TEAD/TEF family of transcription factors, and the coactivator Yorkie (Yki) (21–24). The Yki-Sd transcription complex regulates the expression of a group of genes that participate in cell proliferation, survival, cell-cell interaction, and also maintain the steady-state of cell signaling strength (14). The Hpo pathway coordinates cell proliferation and death by controlling the transcription of key regulatory molecules in cell cycle control and apoptosis, such as *1* and , respectively (23–25).

The Hpo pathway is evolutionarily conserved, although this pathway is more complex in mammals (2, 14, 26). Mammalian Mst1 and Mst2, which belong to the germinal center kinase subfamily (GCKII), are closely related to *D* Hpo, sharing 76% sequence identity (27). Both kinases have an N-terminal catalytic domain and a C-terminal coiled coil interaction motif called the SARAH (for Sav/Rassf/Hpo) domain that mediates self-association as well as association with other SARAH domain-containing proteins (28, 29). Recent studies have demonstrated that Mst1/2 play critical roles in organ size control and cancer formation (30–32) and induce apoptosis after stimulation of cell death (33). Although Mst1/2 have been

* N B I C 973 I G 2010CB912101, 2012CB945001, 2011CB943902; N N F C G 30971646, 30971647, 31171394, 31171414; I G 09 J1410900; N K B D I C G 2011CB915502; I C A I G DA01010405 DA01010406.
[S] I F. 1, 6.
1 H I C A I - . I I .: 86-21-54921336; E-I : @ . . .
2 H I C A I - . I I .: 86-21-54921336; E-I : @ . . .

shown to play vital roles, their activation, which includes caspase-dependent cleavage, binding, and autophosphorylation, is poorly understood (34–37). Recent studies have shown that the pleckstrin homology domain leucine-rich repeat protein phosphatases bind Mst1 and activate Mst1 kinase activity (38).

A number of molecules have been identified to act upstream of Hpo, including the atypical cadherin Fat (Ft) (39–43), the FERM proteins Expanded (Ex), Merlin (Mer) and the newly found Kibra (41, 44–50). How these molecules regulate Hpo activity remains unknown. Nonetheless, negative regulation of Hpo activity has been shown recently. For example, the *D* - RASSF ortholog (dRASSF)[3] blocks Hpo kinase activity by competing with Sav for binding (51). Moreover, protein phosphatase 2 complex, identified as a negative regulator of Hpo signaling complex, is recruited to dRASSF and thus prevents Hpo activation during development (52).

Based on three-dimensional structural analysis, human Mst1 was shown to homodimerize through the C-terminal SARAH domain (28), via an antiparallel conformation (53). These findings suggest that the Mst1 kinase activity may be regulated by homodimerization as well as heterodimerization with members of the RASSF tumor suppressor family.

In this study, we demonstrate that both the N-terminal kinase domain and the C-terminal SARAH domain of *D* - Hpo dimerize. Importantly, we showed that the N-terminal dimerization is critical for the intermolecular autophosphorylation of Hpo and its kinase activity, whereas disruption of the dimerization via the SARAH domain has no significant impact on kinase activity. We also identified a novel dimeric interface that is essential for the kinase activity by maintaining the proper homodimerization between kinase domains. Furthermore, we showed that the Hpo activity is regulated by its nucleocytoplasmic translocation.

## EXPERIMENTAL PROCEDURES

*M t t , , D G t* —Hpo point mutations were generated by PCR-based site-directed mutagenesis and verified by DNA sequencing, and all of these cDNA fragments were cloned into the *A* vector. To construct *ttB- A -FLAG-H* wild type and mutant forms, a *A* vector with attB sequence inserted upstream of the UAS-binding sites was used. The - - *2A- K5* (75B1) flies were used to generate Hpo transformants inserted at the 75B1 *ttP* locus (54). Animals were cultured at 25 °C for adult analysis. *BF33* is a null allele (16). Other transgenes and alleles were driven using *GM -G 4* and *M 1096-G 4*. The mosaic analysis with a repressible cell marker (MARCM) analysis was done as described by Lee and Luo (55). The genotypes for generating clones expressing Hpo variants were *-FLP/+, F 42D BF33/F 42D t -G 80*, and *A -FLAG-H - t /t -G 4 A -GFP*.

[3] : A F, *Drosophila* A F; MA CM, I ; LMB, I B; I , I - ; NE , ; KD, - ; CF , - ; CF A , CF F ; CF B , CF F .

*C C t , t , I t t , t- B t A* —S2 cells were cultured in *D* Schneider's medium (Invitrogen) with 10% fetal bovine serum, 100 units/ml penicillin, and 100 mg/ml streptomycin. Plasmid transfection was carried out using Lipofectamine according to the manufacturer's instructions. A ubiquitin-Gal4 construct was co-transfected with the *A* expression vector for all of the transfection experiments. Immunoprecipitation and Western blot analyses were performed according to standard protocols as described previously (24). To detect phosphorylated Hpo mutants in SDS-PAGE, Phos-Tag AAL-107 (FMS Laboratory) was used according to the manufacturer's instructions. The Phos-Tag is a phosphate binding compound that, when incorporated into polyacrylamide gels, can result in an exaggerated mobility shift for phosphorylated proteins, dependent upon the degree of phosphorylation (56). S2 cells were treated with leptomycin B (LMB; Calbiochem) at 10 ng/ml for 2 h. Antibodies used in this study were as follows: rabbit anti-phospho-Mst1/Mst2/Hpo (Thr-183 of Mst1, Thr-180 of Mst2, Thr-195 of Hpo) antibody (Cell Signaling Technology), mouse anti-FLAG (Sigma), and mouse anti-Myc (Santa Cruz Biotechnology, Inc., Santa Cruz, CA).

*C F t t* —S2 cells were washed three times with chilled phosphate-buffered saline (PBS) and resuspended in 5 volumes of fresh ice-cold hypotonic cell lysis buffer (10 mM Hepes (pH 7.90), 1.5 mM $MgCl_2$, 10 mM KCl) supplemented just before use with 0.5 mM DTT and mixture (Sigma). After incubation on ice for 10 min, the swollen cells were Dounce homogenized until all cells were visibly lysed. The resulting lysate was centrifuged at 4 °C for 7 min at 1,000 × . The supernatant (combined cytoplasmic and membrane fractions) was removed. The pelleted nuclei were recentrifuged at 4 °C at 20,000 × for 20 min to further remove contaminating cytoplasmic and membrane proteins.

*L A* —Cells were cultured in 24-well plates and co-transfected with 15 ng of the - luciferase reporter as a normalization control and 300 ng of *3× 2-L* firefly luciferase reporter (24) using Lipofectamine. Cells were incubated for 48 h after transfection, and then the Dual-Luciferase measurements were performed in triplicate using the Dual-Glo™ luciferase assay system (Promega) according to the manufacturer's instructions. To induce Hpo dimerization in the S2 cell, the ARGENT™ regulated homodimerization kit was used.

*I t* —Immunostaining of imaginal discs and S2 cells was carried out as described (24). Primary antibodies used in this work include mouse anti-FLAG (Sigma), mouse anti-Myc (Sigma), mouse anti-HA (Sigma), rabbit anti-Hpo (produced by immunizing rabbits with the peptide of Hpo amino acids 352–670), and mouse anti-GFP (Santa Cruz Biotechnology, Inc.).

*G t t - (G ) F P t P - A* —GST fusion proteins were produced in *E* and purified with glutathione-agarose beads. GST fusion protein-loaded beads were incubated with recombinant kinases or cell lysates derived from S2 cells expressing individual kinases at 4 °C for 1.5 h. After the beads were washed three times with

lysis buffer, Western blot analysis was performed with antibodies against tags.

*I t K A* —Cell extracts were prepared from S2 cells and immunoprecipitated with anti-FLAG antibody (Sigma) to obtain FLAG-Hpo mutants. The kinase (Hpo mutants) and substrates (GST-Mats) were incubated in kinase assay buffer (50 mM HEPES, pH 7.4, 60 mM potassium acetate, 10 mM $MgCl_2$, 1 mM DTT, 10 $\mu$M ATP along with 10 $\mu$Ci of [$\gamma$-$^{32}$P]ATP) for 30 min at 30 °C. Reactions were stopped by the addition of SDS sample buffer. Then samples were boiled for 5 min at 100 °C followed by SDS-PAGE and autoradiography.

*F E (F E ) A* —For FRET analysis, cyan fluorescent protein (CFP)- and yellow fluorescent protein (YFP)-tagged constructs were transfected into S2 cells together with an ubi-Gal4 expression vector. Cells were washed with PBS, fixed with 4% formaldehyde for 20 min, and mounted on slides in 80% glycerol. Fluorescence signals were acquired with the ×63 objective of a Leica LAS SP5 confocal microscope. Each data set was based on 10–15 individual cells. In each cell, three to four regions of interest in photobleached area were selected for analysis. The intensity change of CFP was analyzed using the Leica software. The efficiency of FRET was calculated using the formula, FRET% = ((CFPAP − CFPBP)/CFPAP) × 100.

## RESULTS

*C H F H t A t D t* —To identify new Hpo partners, we carried out a yeast two-hybrid screen for Hpo-binding proteins using the noncatalytic C terminus of Hpo (residues 605–669). Interestingly, one clone isolated from the screen contained the same Hpo C-terminal region (residues 579–669). Based on this result and the evidence that the last 60 amino acids of C-terminal SARAH domain are well conserved between *D* Hpo and Mst1/2 (20), we hypothesized that Hpo forms dimers through its putative C-terminal SARAH domain like Mst1/2 (53). To test this, we transfected S2 cells with FLAG- and Myc-tagged full-length Hpo. It has been found that differently tagged full-length Hpo co-immunoprecipitated with each other (Fig. 1*A*). We then tested whether this self-interaction affects Hpo activity via induction of homodimerization of full-length Hpo ($Hpo^{fl}$) using the ARGENT™ regulated homodimerization kit (57, 58). We generated $Hpo^{fl}$ with two FKBP (Fv2) domains, which are used to induce formation of homodimer or multimer when small FKBP ligands AP20187 are present. In S2 cells, co-expression of Yki and Sd synergistically activates the luciferase (Luc) reporter gene (*3× 2-L* ) (24), which is significantly suppressed by the co-expression of wild type Hpo or Fv2-Hpo (Fig. 1*B*, *6* and *8*). Inhibition by Fv2-Hpo but not by the wild type Hpo was enhanced by the addition of the ligand AP20187 (Fig. 1*B*, compare *8* and *9* with *6* and *7*). This piece of evidence indicates that the induction of Hpo homodimer promotes its pathway activity.

To investigate whether Hpo activity is regulated by the homodimerization through its C-terminal SARAH domain, we generated point mutations to specifically disrupt dimerization mediated by the SARAH domain. Based on the solution structure of human Mst1 C terminus (Protein Data Bank entry 2JO8) (53), we modeled the structure of the Hpo C-terminal SARAH domain (supplemental Fig. S1*A*). In agreement with the structure information, we found a critical isoleucine (Ile-634) residue that is essential for Hpo homodimerization. Mutation of this residue to an aspartic acid, I634D, is predicted to disrupt the coiled coil-mediated dimerization. As shown in the co-immunoprecipitation (co-IP) experiments, similar to full-length Hpo, the C-terminal Hpo containing the SARAH domain (amino acids 343–670) forms homodimers, whereas the same region of Hpo carrying the I634D mutation, Hpo-$C^{I634D}$, completely failed to do so (Fig. 1*C*). However, full-length Hpo with the I634D mutation, $Hpo^{I634D}$, retains a weak but significant homodimerization capability (Fig. 1*D*), suggesting that regions other than the SARAH domain also contribute to the homodimerization of Hpo.

The I634D mutation is located within the Sav-binding region of Hpo (amino acids 602–669) (18). Thus, we tested the interaction between $Hpo^{I634D}$ and Sav. Co-IP results showed that $Hpo^{I634D}$ binds wild type Sav (Fig. 1*E*). However, when the Sav SARAH domain mutant $Sav^{L563P}$ (Sav-M), in which the critical leucine residue was mutated to a proline based on modeled structure of SARAH domain, was used in the co-IP experiment, an interaction between Sav-M and $Hpo^{I634D}$ was not detected (Fig. 1*E*). It is known that dRASSF restricts Hpo activity by competing with Sav for binding to Hpo (51). We tested whether the I634D mutation affects the binding between dRASSF and Hpo. As shown in Fig. 1*F*, the I634D mutation reduced the interaction between Hpo and dRASSF.

To directly compare the activity of $Hpo^{I634D}$ with wild type Hpo, we generated transformants using the *C31* integration system to ensure that all of the transgenes were expressed from the same chromosomal location ( *tt* at 75B1) so that position effects on gene expression were eliminated (54). When the transformants were expressed by the wing-specific Gal4 driver *M 1096*, a similar, albeit weaker, Hpo activity was detected in HpoI634D transgenic flies compared with the Hpo wild type flies in the context of the reduction in wing size (Fig. 1, *G I*). Taken together, these results indicate that the dimerization of Hpo mediated by the C-terminal SARAH domain modulates its activity, and disruption of SARAH-mediated dimerization compromises interactions with Sav and dRASSF but does not abolish the activity of Hpo.

*N E t (NE ) t H C A I t t B F t H* —The Hpo kinase cascade promotes Yki cytoplasmic accumulation during growth regulation, and the overexpressed Hpo was detected mainly in the cytoplasm (Fig. 2*A*). In S2 cells, transfection of $Hpo^{L619P}$, a mutant incapable of forming a SARAH domain dimer based on our prediction from the modeled structure (supplemental Fig. S1*A*), resulted in the increased nuclear localization of $Hpo^{L619P}$ compared with the wild type Hpo (Fig. 2, compare *B* with *A*). No evidence of Hpo nuclear-cytoplasmic translocation has been shown before; thus, we treated the cells with LMB, a specific inhibitor of nuclear export mediated by leucine-rich NES (59), to examine whether the nucleus-cytoplasm shuttling of Hpo is regulated by the nuclear export pathway. The leucine-rich NES is a highly conserved sequence used

FIG E 1. **Homo- and heterotypic interactions of the Hpo SARAH domain.** *A*, FLAG-H M -H I I . 2 . FLAG- M -H I I -FLAG -M . (*WB*) *left panel*. *B*, 2 H F 2-H , , *3×Sd2-Luc* , D -L . *Error bars*, .D. ( ). *C*, H -I634D-C ( I 343, 670) I634D C- I A AH I I . *arrow*, I G . *D*, - H I634D . *E*, M - -M - FLAG- H H I634D, 2 . *Sav-M*, L563 I . B H I634D M - , -M H I634D. *F*, M - A F - FLAG- H H I634D, 2 . *G–J*, I (*G*) I H (*H*), H I I634D (*I*), I NE 1/2 (*J*) *MS1096*.

by a variety of proteins to facilitate their export from the nucleus to the cytoplasm, and is important in regulating protein function by affecting proteins' subcellular localization (60). After 2 h of LMB treatment, as shown in Fig. 2, *A′* and *B′*, the wild type Hpo accumulated in the nucleus, whereas the nuclear accumulation of $Hpo^{L619P}$ was more predominant. These results indicate that a functional NES(s) exists within the Hpo C-terminal SARAH domain. Sequence analysis of Hpo reveals that Hpo contains two potential leucine-rich NES-like sequences (NES1, amino acids 425–434; NES2, amino acids 610–619), and the L619P mutation lies within the NES2 region (Fig. 3*C*). We mutated the hydrophobic residues to an alanine

FIG. E 2. **Hpo C terminus contains two functional NESs.** *A–B′*, 2 H H L619 I -FLAG .F LMB I 2 , LMB 10 /I 2 .N DA I (*blue*). *C D*, H NE 1/2 I H -N 2 LMB I . *E F*, I FLAG- H - 189A NE 1/2 *MS1096*, I I -FLAG (*green*) . *G–H′*, I (*G G′*) *UAS-exportin RNAi* (*H H′*) *MS1096*, I I -H H (*green*) DA I (*blue*) . *I*, (*N*) I (*C*) 2 H H NE 1/2 LMB (10 /I , 2 ) (*WB*) FLAG . H (*N/C*) *below* . *J*, *3×Sd2-Luc* I H H NE 1/2 2 .

or a proline (L429A, I434A, and L619P) in both NES1/NES2 regions and investigated the subcellular localization of the mutant forms. Hpo$^{NES1/2}$ was distributed throughout the cytoplasm and nucleus (Fig. 2*C*). To confirm the nucleocytoplasmic shuttling of Hpo, S2 cells were transfected with the wild type Hpo or Hpo$^{NES1/2}$. Cytoplasmic and nuclear fractions from the cell extracts were collected. Western analysis revealed that the wild type Hpo was found primarily in the cytoplasmic fraction, and the Hpo$^{NES1/2}$ was equally distributed in both fractions (Fig. 2*I*). Treatment with LMB promotes the accumulation of the wild type Hpo in the nucleus (Fig. 2*I*). These results suggest that both NES sequences are functional.

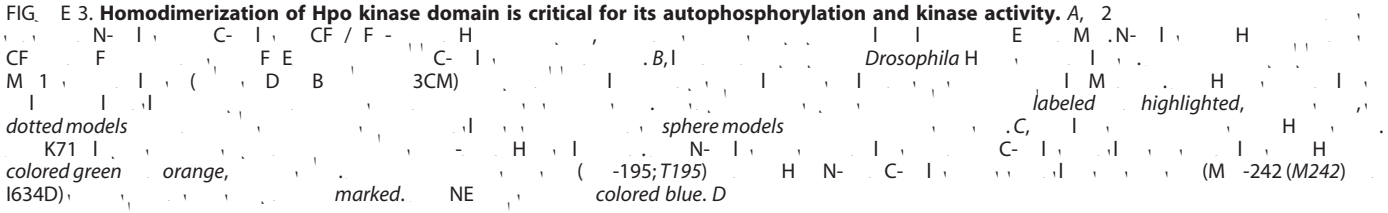

FIG. E 3. **Homodimerization of Hpo kinase domain is critical for its autophosphorylation and kinase activity.** *A*, 2 N- I C- I CF / F - H , I I E M .N- I H CF F F E C- I . *B*, I *Drosophila* H I . M 1 I ( D B 3CM) I I I I M . H I I I I *labeled highlighted*, *dotted models* I *sphere models* .*C*, I H . K71 I - H I . N- I I C- I I I H *colored green orange*, . ( -195; *T195*) H N- C- I I (M -242 (*M242*) I634D) *marked*. NE *colored blue*. *D*

In *D* , Hpo$^{NES1/2}$ overexpressed by *M 1096-G 4* in wing discs exhibited enhanced nuclear accumulation when compared with the overexpressed HpoT189A mutant (described below), which showed a staining pattern similar to that of the wild type Hpo (Fig. 2, *E* and *F*). We further checked the localization of endogenous Hpo when the RNAi transgene for exportin (dCRM1) was overexpressed. Exportin knockdown by RNAi resulted in nuclear accumulation of endogenous Hpo (Fig. 2, compare *H* with *G*).

Next, we examined the functional activity of Hpo$^{NES1/2}$ by luciferase assay using S2 cells. Coexpression of Hpo$^{NES1/2}$ together with Sd and Yki caused a slight decrease in luciferase reporter activity in contrast to the dramatic response elicited by the wild type Hpo (Fig. 2*J*). Expression of Hpo$^{NES1/2}$ in *D* - wing discs resulted in a similar phenotype to the *M 1096* control (Fig. 1*J*′ and supplemental Fig. S1*B*), which suggested that Hpo in the nucleus lost most of its signaling activity, and the regulation of Hpo localization is important for its biological function. Taken together, the C-terminal SARAH domain regulates the Hpo activity via its dimerization and modulation on Hpo nucleocytoplasmic translocation.

*N-t H t H I C t It K A t t B F t* —Because full-length Hpo$^{I634D}$ still dimerizes to a certain degree, we speculated that the N-terminal kinase domain also contributes to the homodimerization of Hpo. To further investigate this, we

employed the FRET assay, which measures the transfer of energy between YFP and CFP to detect protein-protein interaction (61). Two pairs of fusion proteins with CFP/YFP either fused to the N terminus ($CFP^N$-Hpo/$YFP^N$-Hpo) or to the C terminus (Hpo-$CFP^C$/Hpo-$YFP^C$) of the wild type Hpo were generated to examine the interactions of the N or the C terminus by performing FRET analysis in S2 cells. We observed significant FRET between $CFP^N$-Hpo and $YFP^N$-Hpo (~3.93%), which was further increased (~7.59%) when upstream regulators of Hpo, Ex and Mer, were coexpressed (Fig. 3*A* and supplemental Fig. S2). We also observed high FRET between Hpo-$CFP^C$ and Hpo-$YFP^C$, and the change in FRET signals of the Hpo C terminus was not as dramatic as that of the Hpo N terminus with co-expression of Ex and Mer (Fig. 3*A* and supplemental Fig. S2). GST pull-down and immunoprecipitation experiments confirmed that the Hpo N-terminal kinase domain (amino acids 1–342) interacts with itself or endogenous Hpo (supplemental Fig. S3, *A* and *B*), a result in agreement with the recent crystallographic studies of Mst1, Mst3, and Mst4 kinase domains (27). These observations suggested that *D* - Hpo N-terminal kinase domains indeed form homodimers facilitated by the upstream regulators. On the other hand, homodimers formed by the Hpo C-terminal SARAH domains showed only subtle conformational change upon activation.

Because Hpo and Mst1 share over 70% sequence identity in their N-terminal region, we modeled a three-dimensional structure of the Hpo kinase domain (amino acids 1–278) based on the crystal structure of the Mst1 kinase domain (Protein Data Bank entry 3CM). In the modeled dimer of Hpo kinase domains, the $\alpha$H helix and part of the preceding loop of one molecule dock into the active cleft of the other, forming mainly hydrophobic intermolecular contacts with its $\alpha$C helix, activation loop, and $\alpha$H helix (Fig. 3*B*). The homodimeric interface may help maintain an active conformation for full activation of Hpo kinase. Conformational perturbation introduced by point mutation or deletion within this region is expected to affect Hpo kinase activity.

Based on the structural analysis, we first made a deletion form of the Hpo kinase domain (Hpo-$N^{\Delta 238-246}$

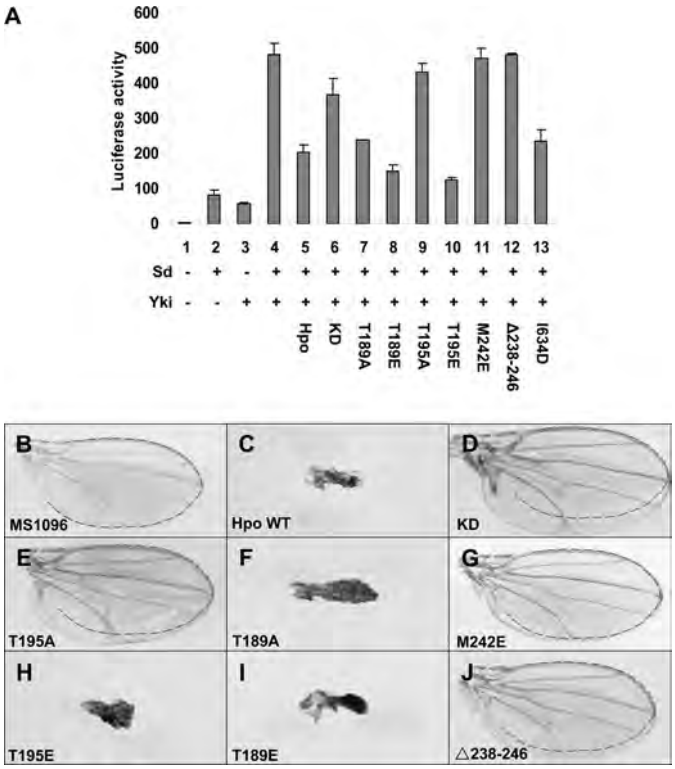


FIG. E 4. **Homodimerization of Hpo kinase domain is critical for its function in growth control.** *A*, 2 H H , , , *3×Sd2-Luc* , D -L . *Error bars*, .D. *B–J*, I (*B*) I H (*C*) H (*D–J*) *MS1096*. *dotted lines* *MS1096* .

protein as a substrate (63). Results showed that wild type Hpo undergoes autophosphorylation and phosphorylates the substrate GST-Mats, whereas the kinase-dead mutation of Hpo, K71R, completely abolished its catalytic activity (Fig. 3*F*). Both HpoT189A and HpoT189E mutants remained as active as the wild type Hpo (Fig. 3*F*, *5* and *6*). The HpoT195A mutant totally lost its kinase activity, but the HpoT195E mutant retained catalytic activity, albeit less potent than the wild type Hpo. The HpoM242E and Hpo$^{\Delta 238-246}$ mutants were completely inactive. On the other hand, the HpoI634D mutant showed slightly reduced kinase activity when compared with the wild type Hpo (Fig. 3*F*, compare *11* and *3*). Collectively, these results suggested that the Hpo catalytic activity depends on its Thr-195 autophosphorylation, and the N-terminal dimeric conformation is crucial for its kinase activity. The Hpo C-terminal dimerization alters its catalytic activity, possibly in a manner of inducing the N-terminal dimeric conformation or changing the substrate specificity. Of note, the HpoT195E mutant showed less activity *t* , most likely due to the fact that the mutation does not fully mimic the Thr-195 phosphorylation and therefore is not optimal for full activation.

*I A t t H t D - t G t I t t t H t* —We then investigated whether these Hpo variants have similar functional defects . Co-transfection of T195A, Δ238–246, M242E, or the Hpo KD together with Sd and Yki failed to suppress the luciferase activity induced by Yki-Sd (Fig. 4*A*). Conversely, the HpoT189A, HpoT189E, and HpoT195E mutants all showed strong Hpo activity (Fig. 4*A*, *7*, *8*, and *10*). On the other hand, HpoI634D mutant was not as effective as the wild type Hpo to suppress Yki-Sd (Fig. 4*A*, *13*). Thus, consistent with earlier *t* kinase assays, Hpo activity is dependent on autophosphorylation at Thr-195 and dimerization. The N-terminal dimerization appears to be more critical than the C-terminal dimerization because disruption of the C-terminal coiled coil-mediated dimerization only partially affects the Hippo activity.

To further confirm whether the N-terminal dimerization is important for Hpo activation, we engineered hybrid proteins by fusing Hpo N-terminal variants with Fv2 protein to test whether induced N-terminal dimerization increases pathway activity in the absence of Hpo C terminus using luciferase assays. As shown in supplemental Fig. S5 ( *4 9*), the enhanced dimerization induces higher activity mediated by the Hpo kinase domain with Fv2 after treatment with AP20187. Among the other hybrid variants, only the Hpo variant N-T195E-Fv2 showed inducible activity, but not the ones carrying M242E or T195A mutations (supplemental Fig. S5). These results suggested that the induced dimer enhances the Hpo kinase activity.

Next, we compared the activity of these Hpo variants in *D* - by overexpression using transgenic flies. To ensure that the transgenes were expressed at the same expression level, all of the transformants were generated by using the *C31* integration system (54). Driven by wing-specific Gal4 driver *M 1096*, Hpo variants carrying T189A, T189E, or T195E mutations caused small and shrunken wings similarly as the wild type Hpo (Fig. 4, *C*, *F*, *H*, and *I*, and supplemental Fig. S6*J*), suggesting that they possess similar activity as the wild type. In contrast, we found that overexpression of Hpo variants carrying M242E or Δ238–246 resulted in a slight increase in wing size, similar to the observations in animals overexpressing HpoT195A (Fig. 4, *E*, *G*, and *J*, and supplemental Fig. S6*J*). Last but not least, only the KD form resulted in significant enlargement of the wings compared with the *M 1096* control (Fig. 4, *B* and *D*, and supplemental Fig. S6*J*).

We further investigated Hpo activities using a genetic interaction assay with Yki in *D* eyes. Overexpression of *A* - posterior to the morphogenetic furrow using the *GM -G 4* driver (hereafter referred as *GM* - ) resulted in enlarged eyes (Fig. 5 and supplemental Fig. S6; compare Fig. 5*B* and supplemental Fig. S6*B* with Fig. 5*A* and supplemental Fig. S6*A*). Expression of *A* - using *GM -G 4* resulted in 100% lethality at early pupal stage, whereas co-expression of the wild type Hpo and Yki led to small rough eyes (Fig. 5*C* and supplemental Fig. S6*C*). Like the wild type, the HpoT195E overexpression also induces small rough eyes in the *GM* - background; however, the HpoI634D overexpression suppressed the *GM* - overgrowth phenotype, leading to rough eyes (Fig. 5, *F* and *I*, and supplemental Fig. S6, *F* and *I*). On the other hand, co-expression of Hpo KD resulted in a dramatic increase in eye size (Fig. 5*D* and supplemental Fig. S6*D*). Similar but weaker phenotypic enhancement was obtained in flies overexpressing HpoT195A, HpoM242E, or Δ238–246 together with Yki by *GM -G 4* (Fig. 5, *E*, *G*, and *H* and supplemental Fig. S6, *E*, *G*, and *H*). These results convincingly showed that Thr-195 is

FIG. E 5. **Hpo variants genetically interact with Yki.** *A–I*, *GMR* (*A*), *GMR-Gal4 UAS-Yki* (*B*), *GMR-Gal4 UAS-Yki* H (*C*), *GMR-Gal4 UAS-Yki* H KD (*D*), *GMR-Gal4 UAS-Yki* H (*E–I*).

critical for Hpo kinase activity, and the N-terminal dimerization is essential for the Hpo activity. Consistent with the *t* data, our studies confirmed that residues around Met-242 within the region of the Hpo homodimeric interface play an important role in maintaining the active conformation of Hpo kinase because mutations in this region abolish the kinase activity.

*H D t I t P t It A t - t A t t* —To investigate whether the homodimerization of Hpo is also critical for its function after autophosphorylation, we made mutant proteins by combining the Δ238–246 deletion with the mutation T195A or T195E (referred to as T195A-Δ or T195E-Δ, respectively). The T195E-Δ mutant proteins are predicted to be incapable of forming native homodimeric association via the kinase domain, but they contain the mimic autophosphorylation site Thr-195. In luciferase assays, we found that T195E-Δ activity was recovered when compared with the $Hpo^{\Delta 238-246}$ mutant (Fig. 6*A*, compare *8* with *10*), and this activity is similar to, albeit less potent than, the T195E mutant (Fig. 6*A*, compare *8* with *9*). Consistently, driven by wing-specific Gal4 driver *M 1096*, T195E-Δ showed stronger pathway activity compared with Δ238–246 (compare Fig. 6*C* with Fig. 4*J*) but much weaker than that of T195E, which dramatically reduced the wing size (compare Fig. 6*C* with Fig. 4*H*). In contrast, the T195A-Δ and T195A mutants did not show substantially different activities either by luciferase assay or analysis (Fig. 6*A*, compare *6* with *7*; compare Fig. 6*D* with Fig. 4*E*). These results suggested that, although the dimeric interface of the N-terminal kinase domain was deformed by Δ238–246, the HpoT195E-Δ, but not T195A-Δ, was still functional and capable of triggering Hpo signaling. Taking this result together with the results of previous kinase assays, we concluded that the dimerization is the prerequisite of Hpo autophosphorylation at Thr-195 and leads to Hpo activation.

FIG. E 6. **Hpo dimerization is the prerequisite of autophosphorylation and activity.** *A*, 2 H H *3×Sd2-Luc* D -L . Error bars, .D. *B–D*, (*B*) *UAS-Hpo-T195E-Δ* (*C*) *UAS-Hpo-T195A-Δ* (*D*) *MS1096* I .

*A t H t t O t P t H M t t* —To investigate whether these Hpo variants still possess Hpo activity independent of endogenous Hpo , we further tested their ability to rescue the $^{BF33}$ null allele in *D* using the MARCM technique to express these variants in clones mutant for $^{BF33}$(16,55). As shown in Fig. 7, adult eyes carrying $^{BF33}$ mutant clones were overgrown, showing enlarged and folded eyes (Fig. 7*A*). In contrast, wild type Hpo expression in $^{BF33}$ mutant clones was sufficient to inhibit the overgrowth and rescued the adult phenotype, resulting in nearly normal eye size (Fig. 7*B*). Expression of Hpo KD in the $^{BF33}$ clones still caused eyes that were rough and overgrown but somehow less folded compared with the eyes of $^{BF33}$ mosaic flies (Fig. 7*C*). The eyes of the $^{BF33}$ mosaic flies containing Hpo-T195A are even less folded than the eyes of those containing Hpo KD

FIG E 7. **Hpo variants with kinase activity rescue the overgrowth phenotype of *hpo* mutants.** *A–A‴*, *hpo*$^{BF33}$ . *hpo*$^{BF33}$ . *B–F‴*, *hpo*$^{BF33}$ H H . *hpo*$^{BF33}$ H FLAG GF . *A′–F′*, .

(Fig. 7*D*). Moreover, only rough and slightly bigger eyes are shown in the $^{BF33}$ mosaic flies that express Hpo-M242E (Fig. 7*F*). Similar to overexpression of the wild-type Hpo in $^{BF33}$ mosaic flies, overexpression of the HpoT195E completely rescued the eye overgrowth in $^{BF33}$ mosaic flies (Fig. 7*E*). We further compared the size of MARCM clones in the eye imaginal discs. The mosaic clones of $^{BF33}$ were large because of the competitive properties; however, when the wild type Hpo was overexpressed, clones were very small (Fig. 7, compare *B‴* with *A‴*). The Hpo KD and T195A clones were notably larger than the T195E and M242E clones (Fig. 7, compare *C‴* and *D‴* with *E‴* and *F‴*). Furthermore, the T195E clones were apparently larger than the wild type Hpo clones (Fig. 7, compare *E‴* with *B‴*), although they showed a similar adult phenotype, and the M242E clones were smaller than the ones of Hpo KD and T195A (Fig. 7, compare *F‴* with

*C‴* and *D‴*). These sensitive genetic rescue results reveal that the M242E has less reduced activity compared with Hpo KD and T195A mutants.

## DISCUSSION

Previous studies have revealed that Hpo signaling is essential for tissue growth and organ size control in both *D* and vertebrates (14). However, despite the emerging significance of this signaling transduction pathway, the mechanism by which the Hpo kinase is regulated is poorly understood. Based on a combination of structural and functional analyses, our results demonstrate that the autophosphorylation and kinase activation of Hpo depends on its homodimerization, which is mediated by two distinct functional domains. We show that dimerization of the N-terminal kinase domain, which is mediated predominantly by hydrophobic interactions, is essential for Hpo autophosphorylation and its kinase activation, whereas the coiled coil-mediated dimerization of the C-terminal SARAH domain is probably necessary to modulate Hpo function.

Consistent with previous studies of Mst1/2 (28), we found that the dimerization of the Hpo SARAH domain is not essential for its kinase activity. Disruption of the dimerization mediated by the SARAH domain only led to a partial decrease for its autophosphorylation and kinase activity (Fig. 3*E*). It is important to emphasize that although the Hpo SARAH domain seems to be non-essential for autophosphorylation, it may be crucial for regulatory functions based on existing studies of Sav and RASSF in both *D* and mammalian cells (51, 64, 65). Indeed, wild type Hpo always shows higher activity than just the kinase domain because *GM -H* results in 100% lethality at the early pupal stage, but expressing the *GM* - Hpo-kinase domain alone results in a weaker phenotype. Misexpressed HpoI634D in *D* wing results in a discernible change compared with the wild type Hpo (Fig. 1, compare *I* with *H*). It is likely that the strong kinase activity caused by overexpression may conceal the regulatory function of the SARAH domain. Our FRET analysis showed that a higher basal level of interaction between Hpo C termini is detected, compared with that between the Hpo N termini. However, when activated by the upstream signaling, the FRET change between C termini is not as dramatic as that observed for that between the N termini (Fig. 3*A*), suggesting that the SARAH domain may constitutively form dimers, whereas the conformation of the N-terminal dimer is inducible. At this point, we speculate that one possible role of the Hpo C-terminal dimerization is to function as a platform to facilitate the intermolecular association between the N-terminal kinase domains. In addition, it seems that the dimerization of SARAH domain may help to stabilize Hpo because we repeatedly detected that the I634D is less stable than the wild type Hpo when expressed in S2 cells.[4] Our immunoprecipitation data support this point by showing that the FLAG-Hpo-C-I634D barely pulled down the endogenous Hpo (supplemental Fig. S3*B*). Furthermore, the activity of Hpo could be regulated by the dimerization partners, which are recognized by the SARAH domain in the upstream or downstream branches of the Hpo signaling pathway, such as dRASSF and Sav (51). Consistent with this finding, we showed that Hpo and Sav/dRASSF heterodimerize via the conserved C-terminal SARAH domains of both proteins (Fig. 1, *E* and *F*).

Hpo SARAH domain plays a dual role in regulating Hpo activity. Besides the functional regulation of Hpo through homodimerization as well as through heterodimerization with other SARAH-containing partners, the SARAH domain of Hpo participates in the regulation of nucleocytoplasmic distribution of Hpo via a CRM1-dependent nuclear export mechanism. We identified two functional NESs that are both located in the Hpo C-terminal region, including the one located in the SARAH domain (Fig. 3*C*). We showed that the nucleus-cytoplasm shuttling of Hpo is regulated by the nuclear export pathway, and the translocation of Hpo is critical for its functional regulation because the $Hpo^{NES1/2}$ lost most of its signaling activity *t* and (Figs. 1*J* and 2). These findings will bring novel insights to our present functional studies and help to answer questions regarding the importance in regulating nuclear-cytoplasmic translocation of Hpo and the function of Hpo in the nucleus.

The Hpo kinase domain (Hpo-N) shows a diffused localization (Fig. 2*D*) when the Hpo C-terminal part is deleted, and its pathway activity is much lower than the activity of wild type Hpo, which localizes mainly in the cytoplasm (Fig. 2*A*). However, mammalian Mst1 is activated by autophosphorylation and the caspase-dependent cleavage, which releases the active 36-kDa N-terminal kinase domain (34, 36, 66). The active truncated kinase translocates into the nucleus and promotes apoptosis by phosphorylating nuclear substrates (67). Because Hpo does not have the conserved caspase cleavage site, our observation suggested that Hpo may exhibit the growth-suppressive activity mainly in the cytoplasm; therefore, a different mechanism from the mammalian MST needs to be determined. Mammalian Mst1/2 protein was localized predominantly or entirely in the cytoplasm in an LMB-dependent manner (37), and the function of nucleocytoplasmic shuttling of MST1/2 needs to be further studied.

Although considerable progress has been made in investigating the mechanisms of regulation and function of the SARAH domain in the Hpo signaling pathway, much less is known about the activating mechanisms of the N-terminal kinase domain, especially . We performed a structure-function analysis of *D* Hpo based on the modeled three-dimensional structure of Hpo kinase domain. As a result, we identified that Thr-195 is the autophosphorylation site and critical for Hpo kinase activity. More importantly, we demonstrated that the N-terminal kinase domain of Hpo mediates homodimerization independently of the C-terminal SARAH domain and that the dimeric conformation of the kinase domain is essential for intermolecular autophosphorylation. As shown in Fig. 3, *D F*, and supplemental Fig. S3*A*, a point mutation, M242E, which is predicted to interfere with the N-terminal dimeric conformation, resulted in the loss of autophosphorylation and kinase activity but not self-interaction. All of our genetic analyses and genetic interaction data in *D* were consistent with the biochemistry results and supported our findings (Figs. 4 and 5).

[4] .J , L. D , .L , . , .H , . , J. J , . , L. , .

Moreover, overexpression of the deletion form Δ238–246 induces bigger organ size using different drivers in *D* (Figs. 4*J* and 5*H*) compared with M242E (Figs. 4*G* and 5*G*). This is consistent with our prediction that Δ238–246 interferes with the dimeric conformation to an even larger extent and therefore functionally imposes a stronger dominant-negative effect compared with the point mutation M242E. Hpo KD and T195A behaved in a dominant-negative manner because they may nonproductively associate with endogenous Hpo or Sav and block signal activation, whereas overexpressed M242E and Δ238–246 may interfere with endogenous Hpo homodimer, as shown (supplemental Fig. S3*B*), and exhibited similar dominant effects. In addition, we provided evidence that the intermolecular autophosphorylation of Thr-195 is only achieved when its kinase domains are properly dimerized. We propose that the kinase activity of Hpo depends on Thr-195 phosphorylation, whereas proper dimerization of the kinase domain is the prerequisite of its phosphorylation. Thus, once the autophosphorylation happens, the dimerization may not be that critical anymore. As we show in Fig. 6, *A* and *C*, the hybrid form T195E-Δ still possesses pathway activity.

In summary, our biochemical and genetic results demonstrate, for the first time, that homodimerization and nucleocytoplasmic shuttling regulate the biological function of Hpo. The N-terminal dimeric conformation of Hpo is essential for its intermolecular autophosphorylation and kinase activation and organ size control.

*A t t D . , D . C - H , D . M t H , D . H J t t t t.*

## REFERENCES

. , ., , . ( ) . *Cell* **96,**

. , ., , . . ( ) . . *Development* **138,**

. , ., , ., , ., , . . ( ) - . . *Genes Dev.* **24,**

. , . ( ) . *Genes Dev.* **21,**

. , ., , ., , . ( ) . *Fly* **3,**

. , ., , . ( ) . , , . *J. Genet. Genomics* **38,**

. , ., , . ., , ., , ., , ., , . ., , ., , ., , ., , ., , . ., , . ( ) β- - . *Dev. Cell* **18,**

. - , ., , . ., , ., , ., , ., , ., , . ., , . . ( ) - - - . *Genes Dev.* **23,**

. , ., , ., , . ., , ., , ., , ., , ., , ., , . ., , . ., , . . ( ) *in vivo* . *Proc. Natl. Acad. Sci. U.S.A.* **107,** . , ., , . ( ) . *Curr. Biol.* **19,** . , . ., , ., , . ., , ., , . ., , ., , ., , . ., , . . ( ) - - - . *EMBO J.* **17,** . , ., , ., , ., , . ., , ., , ., , . ( ) . *J. Biol. Chem.* **284,** . , ., , . ., , . . ( ) . . *J. Biol. Chem.* **277,** . , . ., , . ( ) - ( ). *J. Biol. Chem.* **277,** . , ., , ., , ., , ., , ., , ., , ., , . ., , . ., , ., , . . ( ) . *Mol. Cell* **38,** . , ., , ., , ., , ., , . ( ) . *Curr. Biol.* **16,** . - , . ., , ., , . ( ) - - . *Proc. Natl. Acad. Sci. U.S.A.* **105,** . , ., , ., , ., , ., , ., , . . ( ) . *Nat. Genet.* **38,** . , . ., , ., , ., , ., , . . ( ) *Drosophila*. *Genetics* **175,** . , ., , ., - , ., , ., , . ., , ., , ., , . ( ) . *Curr. Biol.* **16,** . , ., , ., , ., , ., , . ., , . ( ) . *Dev. Cell* **18,** . , . ., , . . ( ) *Drosophila* . *Curr. Biol.* **16,** . , ., , ., - , ., , ., , ., , ., - , ., , . ( ) . *Nat. Cell Biol.* **8,** . , ., , . ., , ., , . . ( ) - . *Curr. Biol.* **16,** . , . ., , ., , ., , . . ( ) *Drosophila* , , . *Dev. Biol.* **304,** . , ., , ., , ., , ., , . ( ) *Drosophila*. *Dev. Cell* **18,** . , ., , . ., , ., , . ., , . ( ) . *Dev. Cell* **18,** . , ., , ., , . ., , . ( ) *Drosophila* . *Curr. Biol.* **16,** . , . ., , ., , ., , . ., , ., , ., , ., , . ( ) . *Mol. Cell* **39,** . , ., , . ., , ., , ., , . ., , . ., , . ., , . ( ) - . *Proc. Natl. Acad. Sci. U.S.A.* **104,** . , ., , . ., , ., , ., , . ( ) *Drosophila* - . *Proc. Natl. Acad. Sci. U.S.A.* **104,** . , ., , . ( ) ( ) *Drosophila* . *Trends Neurosci.* **24,** . , ., - , ., , ., , . ( ) - , . *Mol. Cell Proteomics* **5,** . , ., , ., , . ., , ., , . ., , . ., , . ., , . ., , . ., , ., , ., ., , ., , . . ( ) - . *Proc. Natl. Acad. Sci. U.S.A.* **95,** . , ., , ., , ., , . ., , ., , ., , . ., , ., , . . ( ) - . *Proc. Natl. Acad. Sci. U.S.A.* **102,** . , ., , ., , ., , ., , . ., , ., ., , ., , . ( ) . *Proc. Natl. Acad. Sci. U.S.A.* **96,** . , . ., , . ( ) . . *Annu. Rev. Biochem.* **67,** . , . ., , . ., , . . ( ) - ( ) - - ( ) . *Biol. Proced. Online* **6,** . , ., , ., , ., , . ( ) - - . *Curr. Biol.* **16,** . , ., , ., , . . ( ) *Drosophila*. *EMBO J.* **26,** . , ., , ., - , ., , . ( ) - , - , , . *Biochem. J.* **381,** . , . ., , . ., , . . ( ) , , - , - . *FEBS J.* **273,** . , . ., , ., , ., , ., , . ( ) , , . *J. Biol. Chem.* **276,** . , . ., , ., , ., , ., , ., , . ., , ., , . ., , ., , . . ( ) - . *Cell* **113,**

# Dimerization and Cytoplasmic Localization Regulate Hippo Kinase Signaling Activity in Organ Size Control

Yunyun Jin, Liang Dong, Yi Lu, Wenqing Wu, Qian Hao, Zhaocai Zhou, Jin Jiang, Yun Zhao and Lei Zhang

*J. Biol. Chem. 2012, 287:5784-5796.*
*doi: 10.1074/jbc.M111.310334 originally published online January 3, 2012*

---